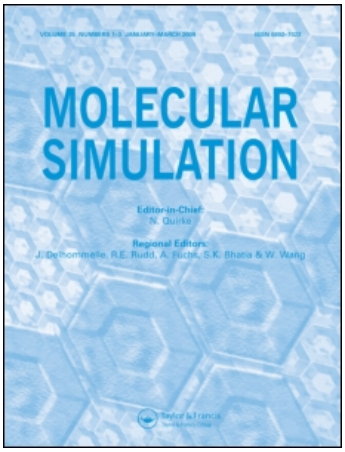

Molecular Simulation
Publication details, including instructions for authors and subscription information:
http://www.informaworld.com/smpp/title~content=t713644482

Ergodicity Range of Nosé-Hoover Thermostat Parameters and Entropy-Related Properties of Model Water Systems

Tatyana Kuznetsova[a]; Bjørn Kvamme[a]
[a] Telemark Institute of Technology, Porsgrunn, Norway

To cite this Article Kuznetsova, Tatyana and Kvamme, Bjørn(1999) 'Ergodicity Range of Nosé-Hoover Thermostat Parameters and Entropy-Related Properties of Model Water Systems', Molecular Simulation, 21: 4, 205 — 225
To link to this Article: DOI: 10.1080/08927029908022062
URL: http://dx.doi.org/10.1080/08927029908022062

Molecular Simulation, 1999, Vol. 21, pp. 205–225
Reprints available directly from the publisher
Photocopying permitted by license only

ERGODICITY RANGE OF NOSÉ-HOOVER THERMOSTAT PARAMETERS AND ENTROPY-RELATED PROPERTIES OF MODEL WATER SYSTEMS

TATYANA KUZNETSOVA and BJØRN KVAMME*

Telemark Institute of Technology, Kjølnes Ring 56, N-3914 Porsgrunn, Norway

(Received June 1998; accepted June 1998)

A model system comprising 108 and 256 TIP4P water molecules was investigated by NVE and NVT molecular dynamics. Translational and rotational temperatures were constrained by Nosé-Hoover thermostats. Our analysis of mode frequencies agree with the conclusions of Nosé. Chaoticity of motion, ergodicity's prerequisite, was violated in case of small thermostat response times. Response times about half again the resonance values resulted in the behavior of both modes matching very closely that of natural ones. A 'hybrid' method of chemical potential calculation due to S. Kumar and never used previously for water was used to calculate the chemical potential. The method yielded a chemical potential lying below the correct specific values, and our simulations indicate that it gives rise to a misleading premature convergence of results. We conclude that while the true usefulness of hybrid method may be restricted to macromolecules, it could also be treated as a convenient mathematical trick.

Keywords: Molecular dynamics; ergodicity; Nosé-Hoover thermostat; chemical potential; water

INTRODUCTION

Recent years have seen the ever-increasing use of molecular dynamics simulations for estimation of thermodynamic properties and phase equilibria. Together with Monte Carlo, molecular dynamics proved to be one of the most powerful tools available to researchers in the field of atomistic simulations. Over the last two decades molecular modeling made a rapid progress from NVE ensembles realized through straightforward application

* Corresponding author.

of the molecular dynamics towards open systems able to exchange energy and matter with surrounding 'reservoirs' [1–4]. Ever since its introduction, the Nosé-Hoover thermostat became a technique widely used to implement molecular dynamics simulations in an NVT ensemble. Molecular dynamics computer simulations (both at constant temperature and constant total energy) have been used extensively to study pure polar liquids, various aqueous solutions, and water interfaces [5–10]. Yet, to our knowledge, no systematic study has been undertaken up till now to analyze the effect of thermostat control parameters on system's ergodicity and thus the legitimacy of calculated key properties in case of dense polar fluids.

The present paper is divided in two parts, first one is an investigation into the ergodicity range of Nosé-Hoover thermostat parameters as applied to TIP4P water, in the second part we revisit the 'hybrid' method of chemical potential calculation due to S. Kumar [11] and never used previously for water.

Our runs used timesteps of 0.5 and 0.25 fs, quite small compared to those of other works [5, 6, 9, 12, 13]. Though too short for production run purposes and leading to accumulation of considerable roundoff errors, timestep of 0.25 fs enables one to investigate the natural frequencies of translational and rotational degrees of freedom with a high degree of certainty. And as our analysis of mode behavior will show, timestep of 0.5 fs is what's needed to integrate the rotational motion with at least 40 points per oscillation period. The analysis of mode frequencies has borne out conclusions and estimates derived from Nosé equations [2]. Simulation details such as intermolecular potentials and equations of motion are given in Appendix.

I. NOSÉ-HOOVER THERMOSTAT PARAMETERS AND ERGODIC PROPERTY OF THE SYSTEM

Since the use of molecular dynamics is dictated in many cases by the desire to obtain dynamic characteristics of the system, any method used to control the temperature must yield canonical distribution not only in coordinate space but velocity space as well. This in its turn raises the problem of the ergodic behavior of the system. While it is universally accepted that even the most straightforward of constant-temperature schemes like velocity scaling will yield a canonical distribution in configurational space, canonical distribution of dynamic properties is a much more difficult problem. Potential

energy is a good example of properties well reproduced by means of velocity scaling, while it would be unreasonable to expect the same for single-particle dynamic properties such as diffusivity or collective phenomena like sound propagation. On the other hand, as the results of our simulations show, lack of canonical distribution in momenta space could lead to differences in potential energy estimates in the case of the Nosé-Hoover thermostat.

Satisfaction of ergodic hypothesis, equality of time and ensemble averages, is necessary to obtain the canonical limiting distribution in phase space. For this equality to be assured the system's time evolution must bring it inevitably from nonequilibrium states to equilibrium ones. Microcanonical distribution of the extended system consisting of the real system plus the thermostats is guaranteed by its quasi-ergodic property (system passing arbitrarily close to all available phase space in the course of time evolution). The latter condition calls for divergence of trajectories separated initially by infinitesimal distance, and this requires chaoticity. NVE, or microcanonical ensemble is chaotic, which implies that its evolution in the momenta space is chaotic too.

We realize, of course, that despite the identity of statistical ensembles in the thermodynamic limit there exist significant differences between kinetic energy fluctuations in microcanonical and canonical ensembles, and thus no degree of resemblance between their corresponding modes should be taken as a guarantee of ergodic behavior of canonical properties. Still, a thermostatted system with translational and rotational degrees of freedom at least as chaotic as in microcanonical ensemble, as well as yielding correct averages of kinetic energy and specific heat, has a good chance to reproduce canonical distribution in both configurational and momenta domains of phase space. It has been shown rigorously [2] that once an equilibrium state has been reached the time evolution of a sufficiently chaotic system will yield canonical averages. But this equilibrium can be made unachievable by the presence of an independent high-frequency mode. The case of molecular fluid gives rise to another issue affecting ergodicity, namely, the interplay between the different modes of motion, translational and rotational in the case of rigid central-force water molecule.

Figures 1 and 2 show the typical behavior of translational and rotational modes in the NVE ensemble. We should draw attention to the highly irregular shape of the waveform indicating a substantial coupling between translational and rotational modes reported previously by others [8] and contributing to the ensemble's ergodicity. We have calculated the periods of translational and rotational modes in the NVE ensemble, the values for two different timesteps agree very well and are equal to 43 and 21 fs, respectively.

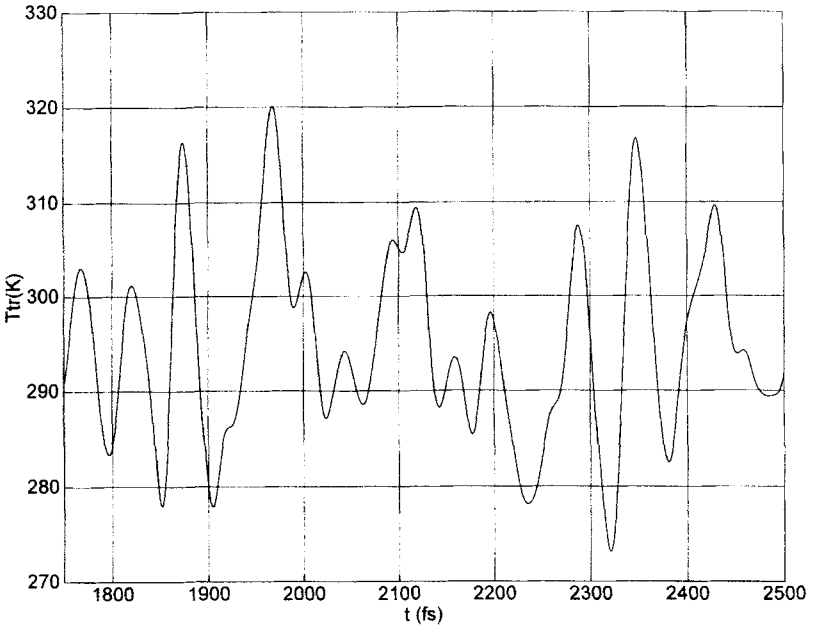

FIGURE 1 Variation of translational temperature in NVE ensemble of 256 TIP4P water molecules. $\tau_{tr} \approx 43$ fs ($dt = 0.25$ fs).

Figure 3 demonstrates that chaoticity of motion, ergodicity's prerequisite, is clearly violated in case of small thermostat response times because of too tight restrictions imposed on the individual degrees of freedom. It is also obvious from the figure that small thermostat masses will severely inhibit mode mixing as well, since the modes will be driven by their own thermostats suppressing any possible interactions. We should also note that temperature fluctuations in this case are much smaller than those corresponding to intermediate and large thermostat response times. The latter proved to be virtually independent of the thermostat mass, as they should be, since the average fluctuation of kinetic energy in a canonical distribution depends only on temperature. Potential energy of the system as a function of thermostat response time for $dt = 0.5$ fs is collected in Table I. It could be seen that once again, values generated by 'ergodic' but not too large thermostat parameters agree very well while differing appreciably from potential energy corresponding to very short and very long response time. We will return to this issue later in the section dealing with chemical potential estimation.

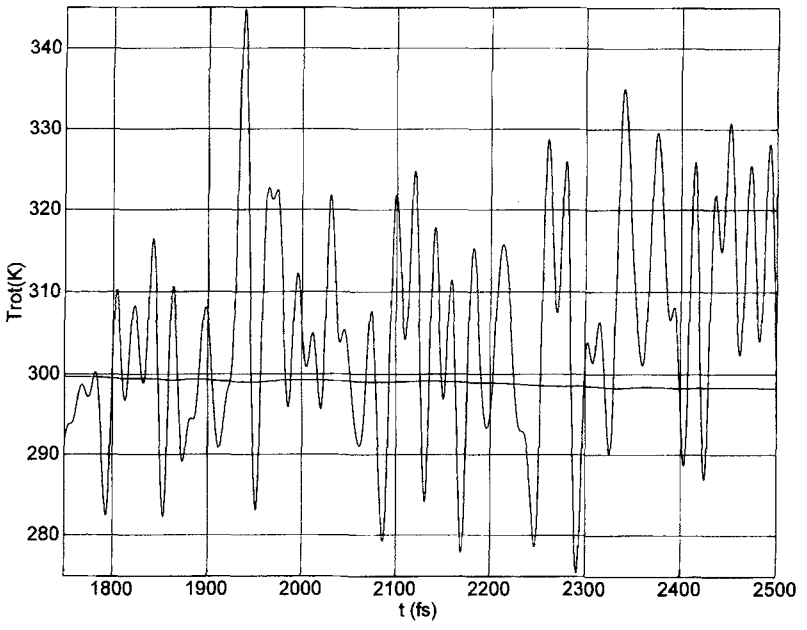

FIGURE 2 Variation of rotational temperature in NVE ensemble of 256 TIP4P water molecules. $\tau_{rot} \approx 21$ fs ($dt = 0.25$ fs).

Performing simulations for two system sizes of molecules has enabled us to see the size dependence of potential energy, $U = -39.4$ kJ/mol for 108 molecules, and -40.8 kJ/mol for $N = 256$. The latter energy agrees well with the previous results for TIP4P water. The former value is higher than internal energies reported by various authors mostly employing constraint schemes like RATTLE and SHAKE. On the other hand, our results could be compared with those of [8] for 500 SPC/E water molecules where the same quarternion treatment of rotational motion was employed (potential energies of SPC/E and TIP4P models differ only by 0.1 kJ/mol [13]. When interpolated to 298 K, their potential energy amounts to -39.3 kJ/mol. We believe this is due to the authors of [12] using the timestep of 1.5 fs, since we have found that while potential energies yielded by timesteps 0.25 and 0.5 fs were practically identical, increasing the integration step beyond 0.5 fs tended to increase the energy.

It's been argued [2] that since the purpose of a thermostat is to provide the transfer of energy between the system and the heat 'bath' the most efficient coupling would be ensured when the thermostat frequency is at resonance with the natural frequencies of the system. Our analysis shows that the

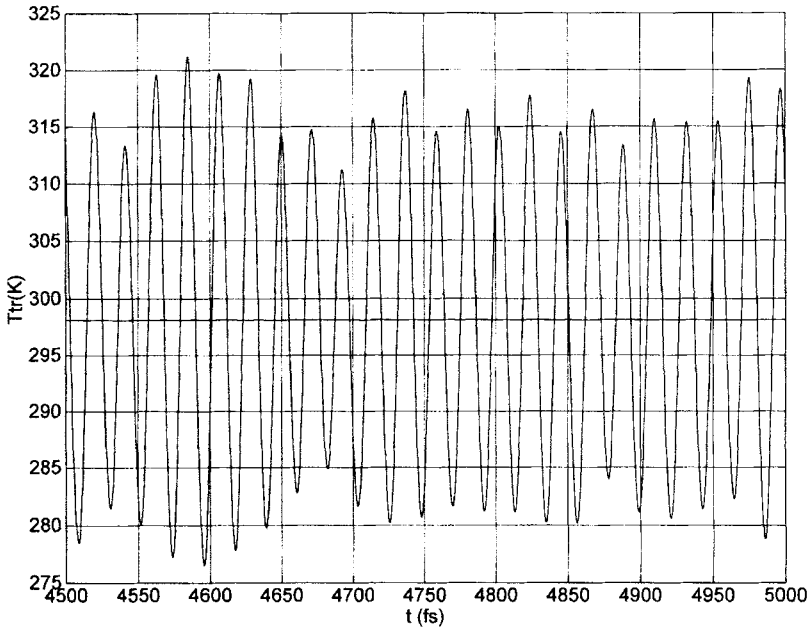

FIGURE 3 Variation of translational temperature in NVT ensemble of 256 thermostatted TIP4P water molecules. $T_{tr} = T_{rot} = 298\,K$, $QT = 10$, $\tau_{tr} \approx 22\,fs$ ($dt = 0.5\,fs$).

TABLE I Potential energy of TIP4P water 298 K as a function of thermostat parameters. $N = 256$. Error bars are indicated in parenthesis

QT*	QTR*	$\langle U \rangle^{\#}$
10.0	1.5	−40.9 (3)
33.0	16.5	−40.8 (4)
76.0	38.0	−40.6 (4)
120.0	60.0	−40.7 (4)
240.0	120.0	−40.6 (4)
1000.0	500.0	−40.4 (4)

* in units of $dt = 0.5\,fs$.
# in units of kJ/mol.

resonance conditions might be far from ideal where the ergodicity considerations are concerned. Consider Figures 1 and 4, their comparison shows striking dissimilarities in the general waveform pattern between natural translational modes and thermostatted ones in case of resonance. Substantial coupling between the modes which is present in the NVE ensemble (see Fig. 1) appears to be absent at resonance, with the complex

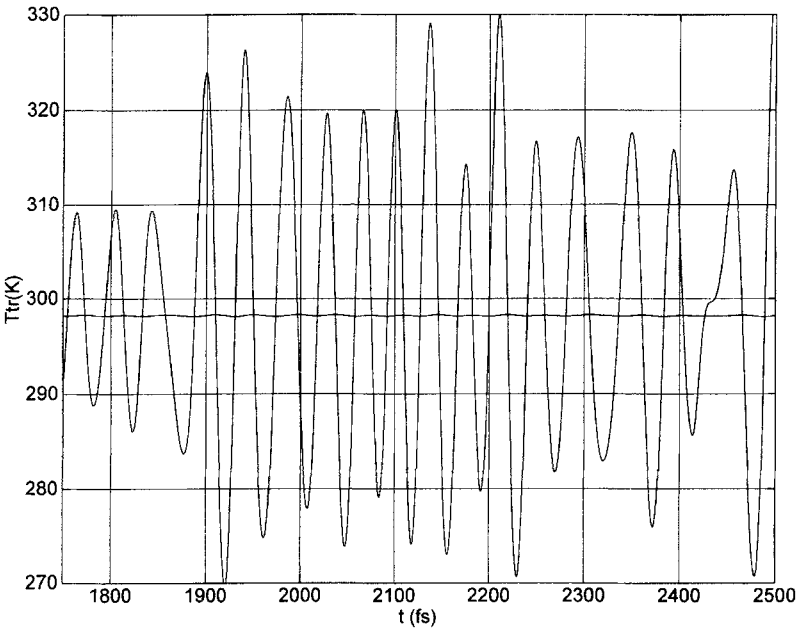

FIGURE 4 Variation of translational temperature in NVT ensemble of 256 thermostatted TIP4P water molecules. $T_{tr} = T_{rot} = 298$ K, $QT = 40$ ($dt = 0.25$ fs).

shape of translational NVE mode substituted by regular sine though with almost identical frequency. While Figure 5 ($QT = 66$, $QTR = 33$, $dt = 0.25$ fs) generated by thermostat response times about half again of their resonance values demonstrates the mode behavior showing a striking resemblance to the natural one. This line of reasoning seems to indicate that thermostat response frequencies should be set somewhat below the resonance values to permit for the proper coupling of translational and rotation modes.

Our analysis of translational and rotational mode frequencies in case of short, intermediate and long thermostat response times follows that of Nosé [2]. According to linearized Eq. (6.6) of [2] valid for small thermostat masses (response time) if τ is the thermostat response time the period associated with the thermostat will be

$$T_1 = \frac{2\pi\tau}{\sqrt{2}} \approx 4.44\tau, \tag{I-1}$$

and since in this case the variation of system's kinetic energy is driven by the thermostat, T_1 will be the its fluctuation period too. Consider Figure 3

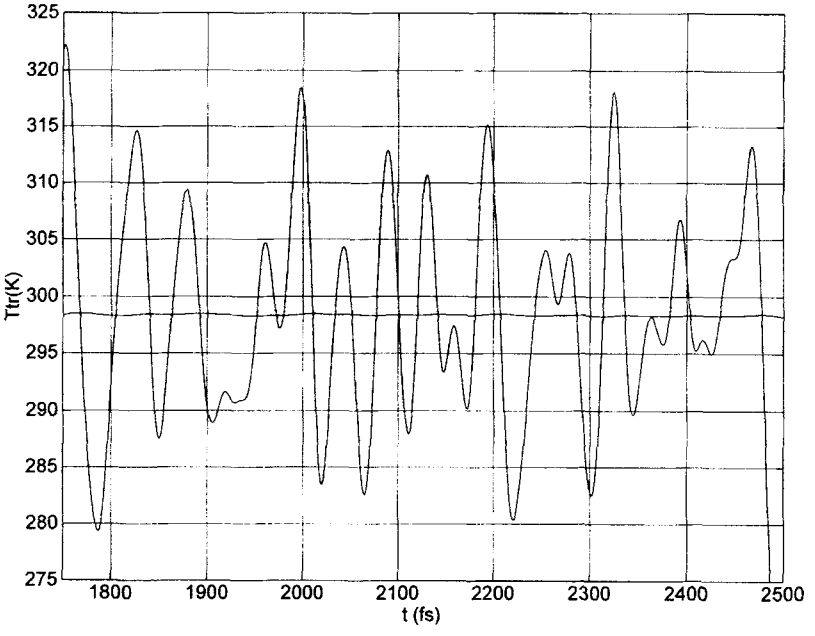

FIGURE 5 Variation of translational temperature in NVT ensemble of 256 thermostatted TIP4P water molecules. $T_{tr} = T_{rot} = 298\,\mathrm{K}$, $QT = 66$ ($dt = 0.25\,\mathrm{fs}$).

($QT = 10$), the period of translational kinetic energy fluctuations is about 22 fs, Eq. (I-1) yields $T_1 = 22\,\mathrm{fs}$, an excellent agreement. Equation (I-1) also holds for rotational mode of Figure 6 where $dt = 0.25\,\mathrm{fs}$ and $QTR = 2.75{:}T_1$ observed from the figure is equal to 2.9 fs, while Eq. (I-1) gives $2.75{*}0.25\,\mathrm{fs}$ $*4.44 = 3.0\,\mathrm{fs}$.

In the opposite case of large thermostat masses when the overall fluctuations of the kinetic energy are those of the canonical ensemble but the fluctuations around the time-dependent fluctuation, $T(t)$, are those of the microcanonical ensemble [2], the period of system's fluctuations will be

$$T_2 = \frac{2\pi\tau}{\sqrt{2}} \left[\frac{2C_v}{gk_B}\right]^{1/2} \tag{I-2}$$

where C_v is the heat capacity, g, number of degrees of freedom. If we assume C_v to be $3Nk_B$, T_2 will be reduced to $2\pi\tau$. The aforementioned superimposition of fluctuations could be clearly observed in Figure 7 ($QTR = 500$, $dt = 0.25\,\mathrm{fs}$). Period T_2 as estimated from Eq. (I-2) will be $500{*}0.25\,\mathrm{fs}{*}$ $2{*}3.1415 = 630\,\mathrm{fs}$. Observed T_2 is about 800 fs. This twenty percent disagreement can be attributed to deviation of water from Dulong-Petit law.

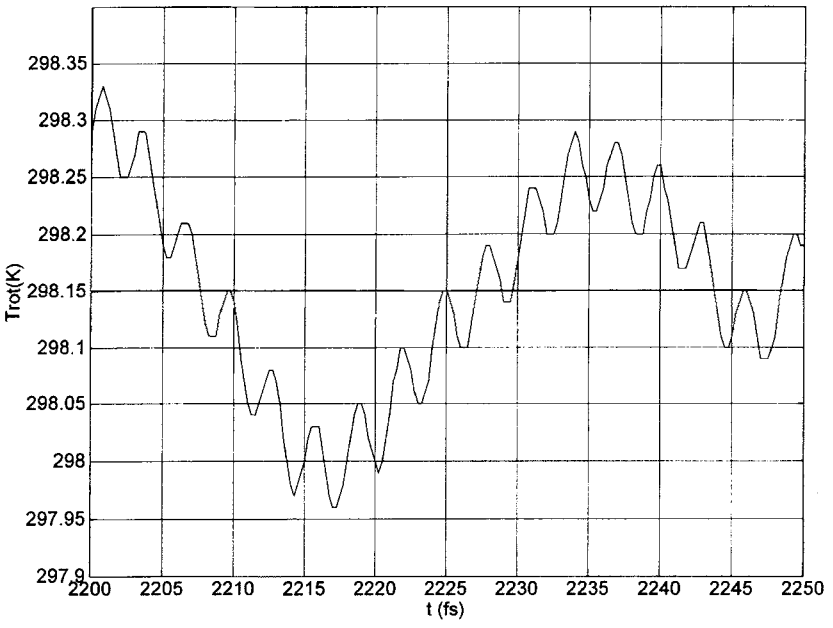

FIGURE 6 Variation of rotational temperature in NVT ensemble of 256 thermostatted TIP4P water molecules. $T_{tr} = T_{rot} = 298\,K$, $QTR = 2.75$ ($dt = 0.25\,fs$). Superimposition of short-period thermostat frequencies ($\tau \approx 3\,fs$) and relatively long-period natural frequencies.

Mixtures of water with various alcohols find numerous applications in different industries making their simulation an important field of study. Separate thermostatting of different molecular species will break the conservation of linear momentum [2]. Theoretically speaking, drastically different geometries of water and alcohol molecules should affect the actual coupling of translational and rotational modes in them. A water molecule is basically symmetric, and its rotation will be governed mainly by changes in electrostatic potential, while any rotation of alcohol molecule will have considerable volumetric effects. On the other hand, when the response time are large enough they do not seem to restrict the proper coupling of modes as shown earlier. We believe that if the corresponding mode frequencies in water and methanol are not too much apart to make thermostatting lax for the highest frequency present, using a single thermostat for water and methanol will be entirely legitimate. With this in mind, we did a series of runs to establish the natural frequencies of methanol represented as a three-site CH3-O-H model (see Appendix) [7]. We have found that the oscillation periods of translational and rotational modes in this methanol model were

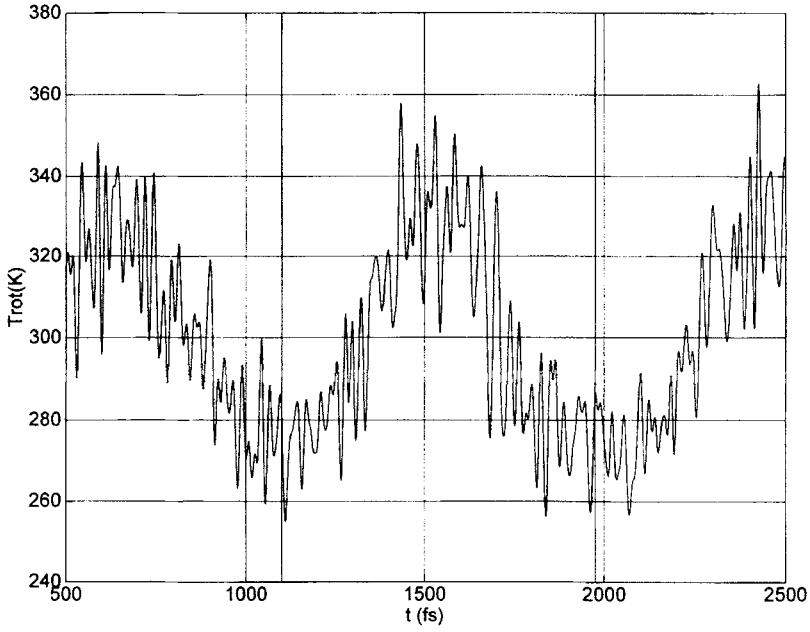

FIGURE 7 Variation of rotational temperature in NVT ensemble of 256 thermostatted TIP4P water molecules. $T_{tr} = T_{rot} = 298\,K$ opposite case. $QTR = 500$ ($dt = 0.25\,fs$). Superimposition of long-period thermostat frequencies and much shorter natural frequencies. See discussion in text.

47 and 25 fs, respectively. The corresponding values for TIP4P water are 44 and 21 fs. Our results support the above conclusion about the validity of properties (both static and dynamic) obtained through application of Nosé-Hoover thermostats to water–alcohol mixtures.

II. HYBRID METHOD FOR CALCULATION OF EXCESS CHEMICAL POTENTIAL

A number of important physical properties like internal energy, heat capacity, diffusion coefficient, or pressure could be expressed as NVE and NVT ensemble averages over the phase-space trajectory. And as such they could be evaluated in the course of a single simulation run with constant parameters. This is possible because these 'mechanical' properties are related to the ratio of two high-dimensional integrals rather than integrals themselves. Entropy and entropy-related functions proves to be a very im-

portant exception. By its very definition entropy depends on the volume of phase space available to the system (its partition function) which makes it very difficult to determine within a canonical ensemble. On the other hand, knowledge of chemical potential and free energy is essential for determination of phase equilibria in chemical reactions and multicomponent systems. This is why considerable effort has been expended by numerous researchers to formulate techniques allowing to determine these thermodynamic functions from computer simulations. Thermodynamic integration, the simplest and perhaps the most reliable of these techniques, requires several simulations to obtain entropic properties of interest. Straightforward application of Widom's particle insertion method [14, 15] is known to fail at high densities due to poor sampling. Various versions of cavity-biased insertion technique were used by several authors to overcome the sampling problem for water and other dense liquids [5, 10].

Extending the system under investigation into a discrete set of balanced subensembles differing in such parameters as temperature, number of particles, or 'ghostliness' of chain gives rise to the method of expanded ensembles [16, 17]. All information necessary for determination of free energy or chemical potential could be extracted in the course of a single simulation run, since the system's evolution takes it from one subensemble to another through a Monte Carlo routine. This approach appears to work even for such exotic system as quantum Heisenberg model [18]. Yet another line of attack could be implemented within the framework of grand canonical ensemble [4, 12, 19] where chemical potential is treated as an input parameter and the number of particle (density) as dynamic variable. After density has been determined for several input values, chemical potential at the density of interest could be estimated by means of interpolation.

On the other hand, while it is the spatial distribution of excess chemical potential which ultimately governs the transport of solutes across biological bilayers [5], permeation of gas mixtures through carbon and silicate membranes [20, 21], and other interfacial phenomena, thermodynamic integration or any other scheme requiring a transition to ideal-gas behavior is not applicable to the majority of such inhomogenous systems stable only within a certain temperature range.

'Hybrid' or modified real particle method was proposed by S. Kumar [11] as a method suitable for calculation of chemical potential at high densities. This technique combines Widom's test particle and the so-called real particle methods and calls for fictious removal and subsequent reinsertion of particles already present in the system. We refer to the original Kumar's papers for arguments and particulars, only providing here the main

equation used to estimate the excess chemical potential

$$\exp(\beta\mu_r) = \frac{\langle \exp(\beta U_{\text{old}}) \rangle_N}{\langle \exp\{\beta(U_{\text{old}} - U_{\text{new}})\} \rangle_N}, \tag{II-1}$$

where β is the inverse of temperature times Boltzmann constant, $1/k_B T$, μ_r-excess chemical potential, U_{old}- potential energy of particle to be reinserted, U_{new}-its new potential energy, angular brackets represent the statistical averages. The hybrid technique can be classified as a 'nondestructive' one since it does not affect the proper time evolution of the system. It was suggested that this method would be particularly advantageous for simulation of macromolecules when a removal of a whole polymer chain is likely to create substantial free space and thus facilitate the reinsertion. Though tested in the original paper on Lennard-Jones particles and proved to yield good results at densities up to 1.1 and T^* down to 0.7, the hybrid technique was neglected from then on. To the best of our knowledge, this is the first reported application of Kumar's hybrid technique for molecular liquid at high densities.

Hybrid technique was applied to the above described model system at 273 K and 298 K. Most of the calculations were made with the thermostat parameters set to their optimum values determined previously but a series of simulations used parameters outside of ergodicity range to ascertain the possible implications.

The 'instant' chemical potentials provided by the method proved to be depend heavily on the number of insertions, an expected feature shared with the test particle method, and particular molecule chosen for removal and reinsertion. The former consideration results in the necessity to determine the 'saturation' number of insertions. Figure 8 shows the estimates of chemical potential for the same configuration and varying number of insertion points. Evidently at least 10,000 or even 20,000 insertion points are needed for any meaningful calculation of chemical potential.

The latter dependence is unique to the hybrid technique. In an attempt to explore this issue we compared 'instant' chemical potentials generated by selecting in turn each molecule in the given configuration. Reinsertion points were the same for all the molecules. Figure 9 provides the resultant plots for configurations 3,000 steps apart and 10,000 reinsertion points at $T =$ 273.15 K. One can see that the averaged instant chemical potential behaves much better that the 'single-molecule' one, with the difference between two configurations anticorrelated with the difference in internal energies. In Figure 10 we present a similar plot in case of 5,000 and 10,000 insertions within a configuration at 293.15 K.

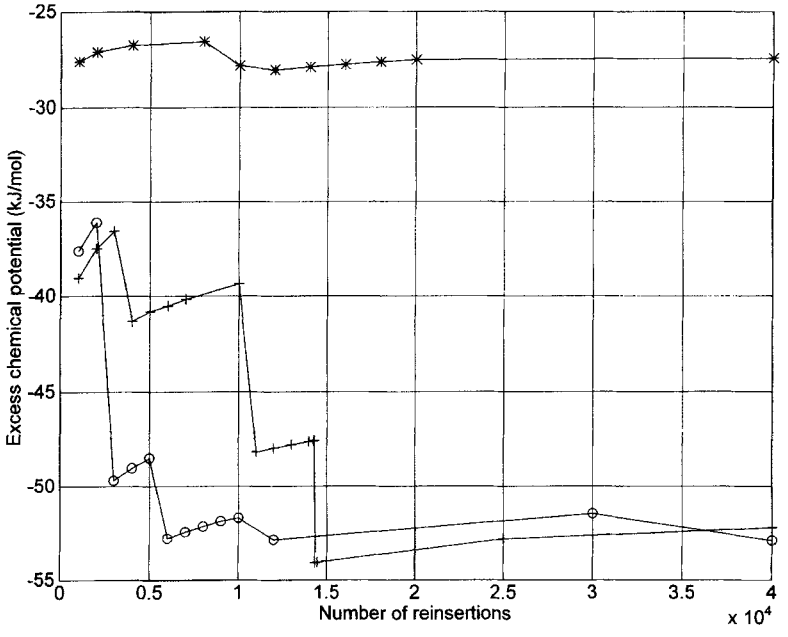

FIGURE 8 'Instant' chemical potential of different configurations *versus* reinsertion number. $T = 273.15$ K, $N = 108$; $*$ – Configuration I; $+$ – Hybrid real particle. Configuration II; o – Configuration III.

As one can see from the figures, hybrid method proved to yield chemical potentials lying below both experimental and model-specific values, and our simulations indicate that it may give rise to a 'premature' convergence of results (Fig. 11). Increasing the number of insertions plunges the chemical potential below the correct value (−22.2 kJ/mol according to [22]). We have come to conclusion that while the true usefulness of hybrid method may well be restricted to macromolecules, it could also be treated as a sort of convenient mathematical trick enabling one, once the 'correct' density of reinsertion points has been determined for a system at 'reference' temperature, to estimate chemical potential at different temperatures and system sizes. This suggestion implies a fortuous cancellation of errors and is not as straightforward as it seems since the strength of hybrid method lies in the fact that removing a molecule will leave a 'hole' where it could be subsequently reinserted without any significant energy penalty. And in case of water, a dense liquid, the relative volume of freed space and thus will be an inverse function of the number of molecules. Thus increasing the number of reinsertion points at constant reinsertion density should not increase the

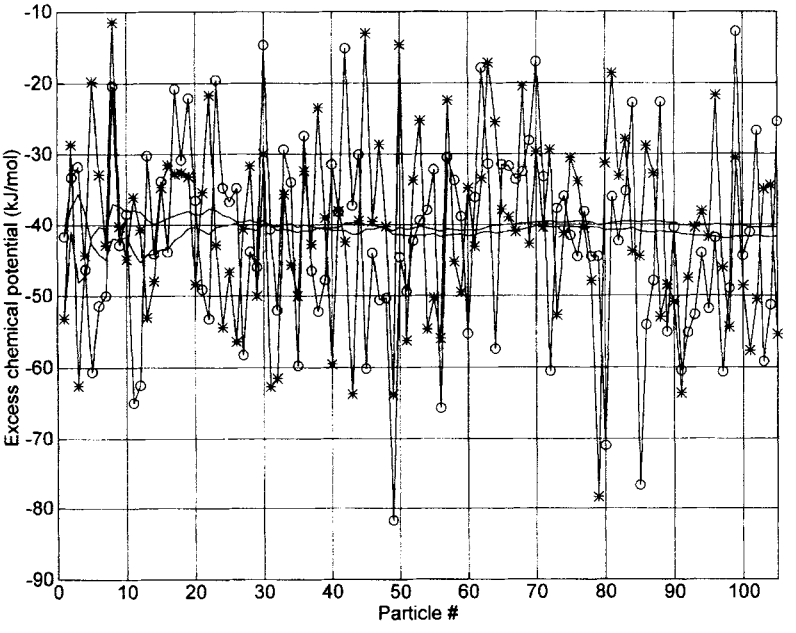

FIGURE 9 System-averaged 'instant' chemical potential. Reinsertion number 10,000. Configurations are 3000 MD steps apart. $T = 273.15\,\mathrm{K}$, $N = 108$, $\Delta U_{12} = 0.63\,\mathrm{kJ/mol}$, $\Delta\mu_{12} = -1.3\,\mathrm{kJ/mol}$. See discussion in text.

probability to hit the hole. The plausibility of our suggestion is illustrated in Figure 11. We found that insertion density of 1,000 points yielded the correct chemical potential of TIP4P water in case of 108 molecules. In case of 256 molecules this density translated to 2,370 insertions. And as Figure 11 shows, a very good agreement of chemical potential results have been obtained this way.

Figures 12 and 13 present the comparison of potential energy and chemical potential for 108 water molecules in two drastically different cases representing tight thermostatting and quasi-canonical behavior, respectively. The increase in potential energy brings the decrease in chemical potential. The observed anticorrelation between potential energy and chemical potential, though unsupported by any theoretical conclusions, appears to be also present in case of 'instant' values as noted above, as well as results of other researchers. We refer to Table I of [12] where different masses of particle reservoir resulted in slightly different values of potential energy and chemical potential displaying the same kind of pattern. We should also note that the difference in estimated chemical potential (about

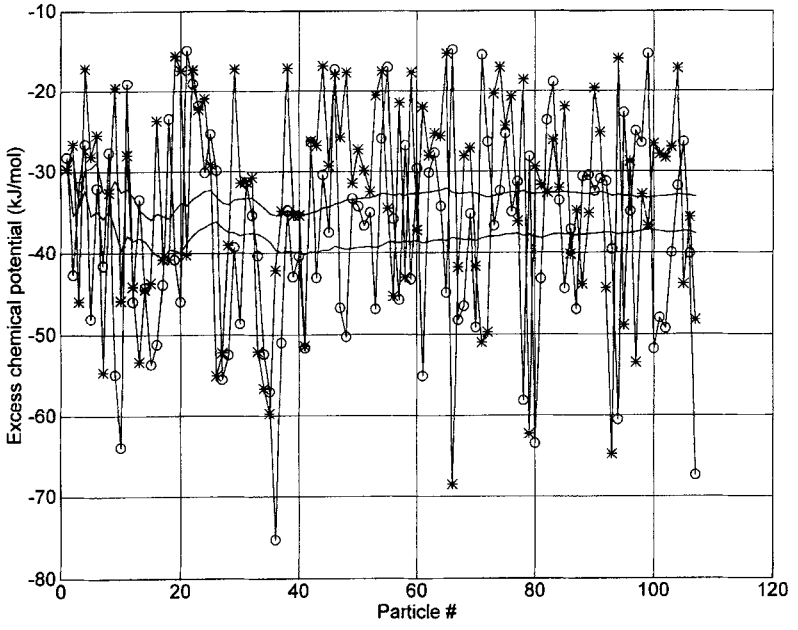

FIGURE 10 System-averaged 'instant' chemical potential for two reinsertion numbers NCOUNT = 5,000 and 10,000.

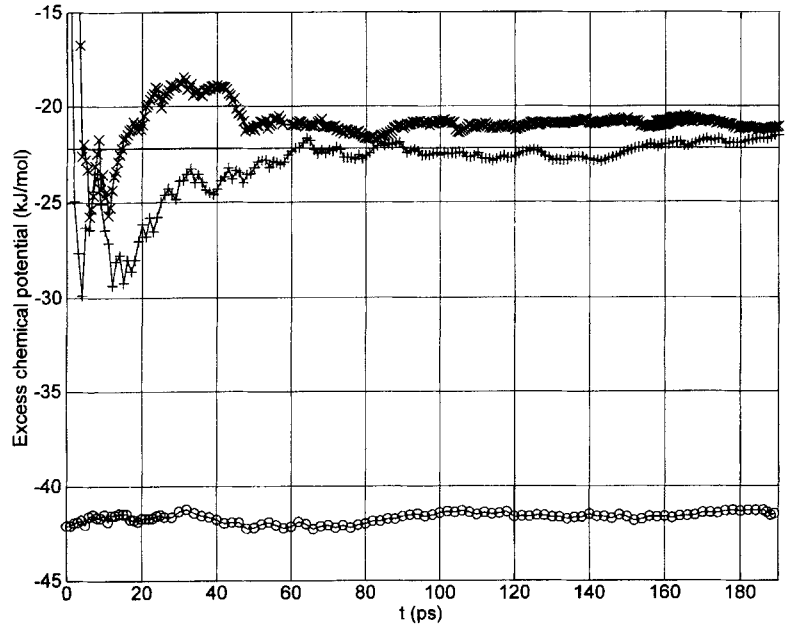

FIGURE 11 Effect of reinsertion point density for 108 and 256 molecules at $T = 298.15$ K, $dt = 0.5$ fs; Straight line – thermodynamic integration results for TIP4P at 300 K [22]; $x - N =$ 108 NCOUNT = 1000; $o - N = 108$ NCOUNT = 20000; $+ - N = 256$ NCOUNT = 2370.

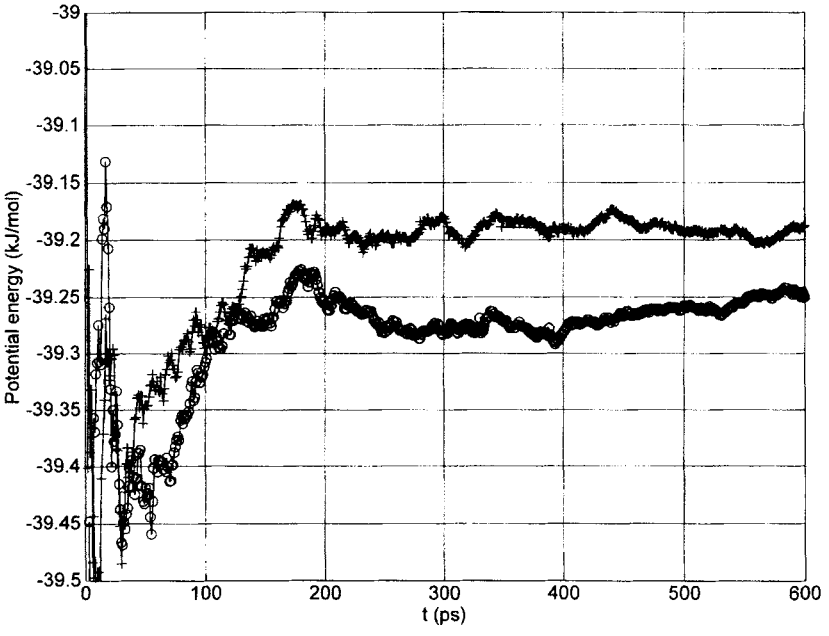

FIGURE 12 Comparison of potential energies for tight and optimum thermostatting. dt = 0.5 fs; Straight line – thermodynamic integration results for TIP4P at 300 K [22]; + – QT = 33, QTR = 16.5; o – QT = 3, QTR = 1.6 (dt = 0.5 fs).

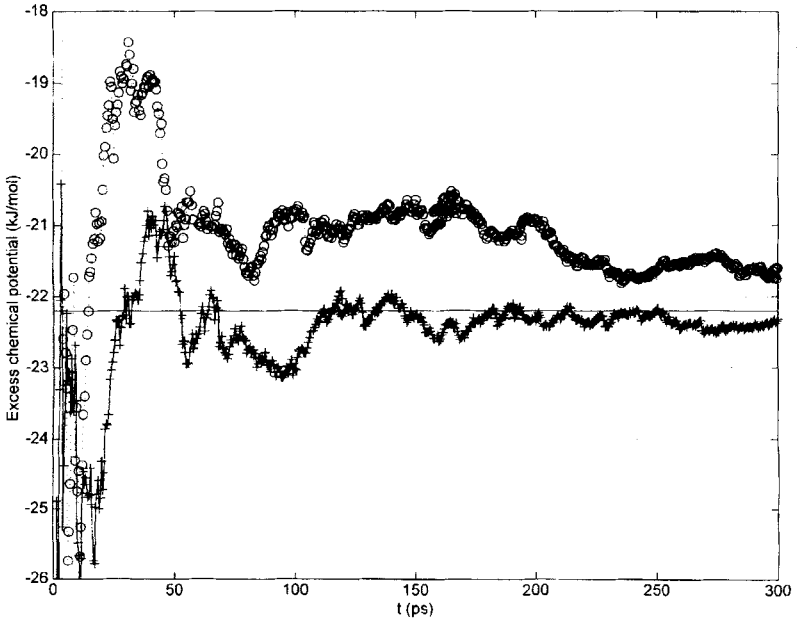

FIGURE 13 Comparison of chemical potentials for tight and optimum thermostatting. See Figure 12 for details.

0.8 kJ/mol) is much larger than even the doubled difference in internal energy (0.05 kJ/mol). We can only suggest here that this is due to relatively large entropy contribution to Gibbs free energy ($A = E-TS$) and chemical potential. Tight thermostatting undoubtedly puts some additional non-physical constraints on the volume of phase space available to the thermostatted system, which will result in entropy decrease and thus an increase in free energy and chemical potential. The mutual position of the two plots in Figure 13 bears out this conclusion, the chemical potential curve corresponding to $QT = 33$ and $QTR = 16.5$ ('ergodic' case) lies well below the curve for $QT = 3$ and $QTR = 1.6$.

III. CONCLUSION

We have used NVE and constant temperature molecular dynamics to determine the ergodicity range of Nosé-Hoover thermostat parameters applied to TIP4P water model. The intrinsic frequencies of translational and rotational modes of motion were found to be 44 and 21 fs, respectively. We have studied the system's behavior under different conditions varying from tight to very loose thermostatting. Our analysis has shown that the system will be quasi-ergodic in a fairly broad range of thermostat parameters, with the period of oscillations yielded by Nose equations and potential energy showing virtually no dependence on thermostat response times. At the same time, we have found that the best match between natural and thermostatted degrees of freedom was achieved when the thermostat frequencies were shifted away from the resonance conditions.

A similar treatment was applied to OPLS methanol. The frequencies of its translational and rotational degrees of freedom were found to lie relative close to those TIP4P water. Coupled with the existence of ergodic 'plateau', this fact enables one to set thermostat parameters in the range assuring ergodic behavior of both components of mixture and thus assure the legitimacy of obtained results.

In the second part of our study we have analyzed the so-called hybrid method for calculation of chemical potential of dense liquids. We have found that it suffered from a 'premature' convergence, with the density of reinsertions yielding correct chemical potential appearing to be size-independent. When the 'saturation' density of reinsertions were determined, the error of hybrid technique was found to be of the same order as that of straightforward test particle technique. The comparison of potential energy and chemical potential in cases of tight thermostatting and ergodic

parameters (performed at 'correct' reinsertion density) has shown that the change in chemical potential is much larger than the change in potential energy (0.8 kJ/mol *versus* 0.05 kJ/mol) which suggests the leading role of entropic contribution, as well as the need to insure the ergodicity of system under simulation before attempting to calculate any of its entropy-related properties.

APPENDIX

The model system comprised 108 and 256 water molecules studied by NVE and NVT molecular dynamics. Our program was modified from McMoldyn package [23]. Water potential used was TIP4P of Jorgensen [24], a rigid model of water where the negative charge, PC, is shifted from the oxygen atom towards the hydrogens along the HOH angle bisector. Methanol was treated as a rigid OPLS molecule with parameters from [7]. We refer the reader to Table II for their respective intermolecular parameters. The intermolecular potential of both water and methanol contained both short-range Lennard-Jones and long-range electrostatic terms:

$$u_{ij} = \sum_{a}^{m} \sum_{b}^{m} \left(\frac{q_i^a q_j^b}{r_{ij}^{ab}} + 4\varepsilon^{ab} \left[\left(\frac{\sigma^{ab}}{r_{ij}^{ab}} \right)^{12} - \left(\frac{\sigma^{ab}}{r_{ij}^{ab}} \right)^{6} \right] \right), \qquad \text{(A1)}$$

where m is the number of sites for the given model (4 for TIP4P water and 3 for OPLS methanol), q_i^a is the charge on the site a of molecule i, r_{ij}^{ab} is the distance between sites a and b located at molecules i and j, ε^{ab} and σ^{ab} are energy and size parameters for the Lennard-Jones interaction between site a and b. Usual mixing rules were applied for interaction of unlike sites.

TABLE II Intermolecular parameter values for TIP4P water and OPLS methanol. PC stands for partial change in TIP4P water, C for united CH_3 site in methanol, $r_{OH} = 0.9572$ Å, $r_{OPC} = 0.1500$ Å, $\alpha_{HOH} = 104.52°$; $r_{CO} = 1.426$ Å, $r_{OH} = 0.9451$ Å, $\alpha_{COH} = 108.53°$

Model	*Site*	ε/k_B [K]	σ [Å]	q [e]
TIP4P	O	78.00	3.15	0
	H	0	0	+0.52
	PC	0	0	−1.04
OPLS	O	87.94	3.083	−0.728
	C	91.15	3.861	+297
	H	0	0	+431

Density of water was set equal to $0.9982\,g/cm^3$, that of methanol to $0.786\,g/cm^3$. Periodic boundary conditions within the starting fcc lattice resulted in the water cell edge length, a, of 14.8 Å and 22.5 Å and cutoff radius $a/2$. Long-range electrostatic interactions were treated by Ewald summation. Translation motion of the center of mass was integrated by means of Toxvaerd's leapfrog formulation [25]. Rotational motion about the center of mass was integrated through explicit leapfrog algorithm employing quarternions [26]. Constant temperature conditions were implemented with translational and rotational temperatures constrained separately by Nosé-Hoover thermostats. The governing equations of motion are presented in (A2) and (A3).

$$\frac{d^2\mathbf{x}}{dt^2} = \frac{\mathbf{F}}{m} \tag{A2a}$$

$$\frac{d\eta_{tr}}{dt} = \frac{\left[\sum m\mathbf{v}^2 - X_{tr}kT_{tr}\right]}{Q_{tr}} \tag{A2b}$$

$$\frac{d\mathbf{j}}{dt} = \mathbf{t} \tag{A3a}$$

$$\frac{d\mathbf{q}}{dt} = \mathbf{Q}\,\hat{\mathbf{w}} \tag{A3b}$$

$$\frac{d\eta_{rot}}{dt} = \frac{\left[\sum \mathbf{jw} - X_{rot}kT_{rot}\right]}{\mathbf{Q}_{rot}} \tag{A3c}$$

where $\mathbf{x}$ are COM coordinates; $\mathbf{F}$ – forces derived from potential (A1); $\mathbf{j}$ – angular momenta; $\mathbf{t}$ – torques; $\mathbf{I}$ – moment of inertia tensor; $\mathbf{w}$ – angular velocity related to angular momentum by $\mathbf{w} = \mathbf{I}^{-1}\mathbf{j}$; $\hat{\mathbf{w}}$ – transposed body-centered angular velocity augmented by a zero to form a four-component vector; $\mathbf{q} = [q_0, q_1, q_2, q_3]^T$ – four-component quarternion representing the orientation of the molecule [26]; $\mathbf{Q}$ – matrix (6c) of [27]; T_{tr} and T_{rot} – required translational and rotational temperatures; η_{tr} and η_{rot} – translational and rotational friction parameters of Hoover formulation [3], X_{tr} and X_{rot} – number of respective degrees of freedom, Q_{tr} and Q_{rot} – thermostat masses determining response times.

Toxvaerd's thermostatted version is realized when the on-step velocities are scaled by factor $\beta = (1 + 1/2\eta)^{1/2}$. Translational and rotational friction parameters are integrated through Eqs. (A2b) and (A3c), respectively, using updated half-step velocities.

Simulations were started from fcc lattice, with discarded equilibration period comprising about 300,000 steps with plain velocity scaling followed by 700,000 thermostatted steps. The validity of the algorithm was checked through the conservation of Hamiltonian with the thermostats switched off. The resulting Hamiltonian curve had the shape of a series of 'plateaus' interspaced by transition zones corresponding to a molecule going beyond the cutoff radius. The overall drift of total energy observed over the period of 5 ps amounted to 0.5% per picosecond.

References

[1] Andersen, H. C. (1980). "Molecular Dynamics Simulations at Constant Pressure and/or Temperature", *J. Chem. Phys.*, **72**, 2384.

[2] Nosé, S. (1991). "Constant Temperature Molecular Dynamics Methods", *Progr. Theor. Phys.*, **103**, 1.

[3] Hoover, W. G. (1985). "Canonical Dynamics: Equilibrium Phase-Space Distribution", *Phys. Rev. A*, **31**, 1695.

[4] Çagin, T. and Pettitt, B. M. (1991). "Grand molecular dynamics: A method for open systems", *Molecular Simulation*, **6**, 5.

[5] Pohorille, A. and Wilson, M. A. (1996). "Excess chemical potential of small solutes across water-membrane and water-hexane interfaces", *J. Chem. Phys.*, **104**, 3760.

[6] Lynden-Bell, R. M. and Rasaiah, J. C. (1997). "From hydrophobic to hydrophilic behavior: A simulation study of solvation energy and free energy of simple solutes", *J. Chem. Phys.*, **107**, 1981.

[7] van Leeuwen, M. E. (1995). "Molecular simulation of the phase behaviour of polar liquids", *Ph.D. Thesis*, Universityu of Utreicht.

[8] Di Cola, D. and Deriu, A. (1996). "Proton dynamics in supercooled water by molecular dynamics simulations and quasielastic electron scattering", *J. Chem. Phys.*, **104**, 4223.

[9] Alper, H. E. and Levy, R. M. (1989). "Computer simulations of the dielectric properties of water: Studies of the simple point charge and transferrable intermolecular models", *J. Chem. Phys.*, **91**, 1242.

[10] Tamai, Y., Tanaka, H. and Nakahashi, K. (1995). "Molecular design of polymer membranes using molecular simulation technique", *Fluid Phase Equilibria*, **104**, 363.

[11] Kumar, S. (1992). "A modified real particle method for the calculation of the chemical potentials of molecular systems", *J. Chem. Phys.*, **97**, 3550.

[12] Ji, J., Çagin, T. and Pettitt, B. M. (1992). "Dynamic simulations of water at constant chemical potential", *J. Chem. Phys.*, **96**, 1333.

[13] Chialvo, A. A. and Cummings, P. T. (1996). "Microstructure of Ambient and Supercritical Water. Direct comparison between Simulation and Neutron Scattering Experiments", *J. Chem. Phys.*, **100**, 1309.

[14] Widom, B. (1963). "Some topics in the theory of fluids", *J. Chem. Phys.*, **39**, 2808.

[15] Widom, B. (1982). "Potential distribution theory and the statistical mechanics of fluids", *J. Chem. Phys.*, **86**, 869.

[16] Lyubartsev, A. P., Martsinovski, A. A., Shevkunov, S. V. and Vorontsov-Velyaminov, P. N. (1992). "New Approach to Monte-Carlo Calculation of the Free-Energy – Method of Expanded Ensembles", *J. Chem. Phys.*, **96**, 1776.

[17] Escobedo, F. A. and De Pablo, J. J. (1995). "Monte-Carlo Simulation of the Chemical-Potential of Polymers in an Expanded Ensemble", *J. Chem. Phys.*, **103**, 2703.
[18] Kuznetsova, T. V. and Vorontsov-Velyaminov, P. N. (1993). "MC Computation of Free Energy in Quantum Two-Dimensional Heisenberg Ferromagnetic Using Expanded Ensemble Method", *J. Phys.: Cond. Matt.*, **5**, 717.
[19] Lynch, C. G. and Pettitt, B. M. (1997). "Grand canonical ensemble molecular dynamics simulations: Reformulation of extended system dynamics approaches", *J. Chem. Phys.*, **107**, 8594.
[20] Furukawa, S., Shigeta, T. and Nitta, T. (1996). "Non-Equilibrium Molecular Dynamics for Simulating Permeation of Gas Mixtures Through Nanoporous Carbon Membrans", *J. Chem. Eng. Jpn.*, **29**, 725.
[21] Pohl, P. I., Heffelfinger, G. S. and Smith, D. M. (1996). "Molecular dynamics computer simulation of gas permeation in thin silicate membranes", *Molec. Phys.*, **89**, 1725.
[22] Hermans, J., Pathiaseril, A. and Anderson, A. (1988). "Excess Free Energy of Liquids from Molecular Dynamics Simulations. Application to Water Models", *J. Amer. Chem. Soc.*, **110**, 5982.
[23] Laaksonen, A. (1995). MCMOLDYN, Daresbury Laboratory U.K.
[24] Jorgensen, W. L. (1982). "Revised TIPS model for simulation of liquid water and aqueous solutions", *J. Chem. Phys.*, **77**, 4156.
[25] Toxvaerd, S. (1991). "Algorithms for canonial molecular dynamics simulations", *Molec. Phys.*, **72**, 159.
[26] Fincham, D. (1992). "Leapfrog rotational algorithms", *Molecular Simulation*, **8**, 165.
[27] Allen, M. P. and Tildesley, D. J. (1990). "Computer Simulation of Liquids", Clarendon Press, Oxford, pp. 86–90.